Unusual cage rearrangements in ten-vertex *nido*-5,6-dicarbaborane derivatives: an interplay between theory and experiment

Bohumil Štíbr,[†] Josef Holub,[†] Mario Bakardjiev,[†] Paul D. Lane,[⊥,‡] Michael L. McKee,[§] Derek A. Wann,[⊥] and Drahomír Hnyk*[,†]

[†] Institute of Inorganic Chemistry of the ASCR, v.v.i., CZ-250 68 Husinec-Řež.

[⊥] Department of Chemistry, University of York, Heslington, York, U.K. YO10 5DD.

[‡] Current address: School of Engineering and Physical Sciences, Heriot-Watt University, Edinburgh, U.K. EH14 4AS.

[§] Department of Chemistry and Biochemistry, Auburn University, Auburn AL, 36849 U.S.A.

■ AUTHOR INFORMATION

Corresponding Author

* E-mail: hnyk@iic.cas.cz (D.H.)

ABSTRACT: The reaction between selected X-*nido*-5,6-$C_2B_8H_{11}$ compounds (where X = Cl, Br, I) and "proton sponge" [PS; 1,8-bis-(dimethylamino) naphthalene], followed by acidification, results in extensive rearrangement of all cage vertices. Specifically, deprotonation of 7-X-5,6-$C_2B_8H_{11}$ compounds with one equivalent of PS in hexane or CH_2Cl_2 at ambient temperature led to a 7 $\rightarrow$ 10 halogen rearrangement forming of a series of $PSH^+[10\text{-X-}5,6\text{-}C_2B_8H_{10}]^-$ salts. Re-protonation using concentrated H_2SO_4 in CH_2Cl_2 generates a series of neutral carbaboranes 10-X-5,6-$C_2B_8H_{11}$, with the overall 7 $\rightarrow$ 10 conversion being 75, 95, and 100% for X = Cl, Br, I, respectively. Under similar conditions, 4-Cl-5,6-$C_2B_8H_{11}$ gave ~66% conversion to 3-Cl-5,6-$C_2B_8H_{11}$. Since these rearrangements could not be rationalized using the B-vertex swing (BVS) mechanism, new cage rearrangement mechanisms, which are substantiated using DFT calculations, have been proposed. Experimental ^{11}B NMR chemical shifts are well reproduced by the computations; as expected $\delta(^{11}B)$ for B(10) atoms in derivatives with X = Br, I are heavily affected by spin-orbit coupling.

KEYWORDS: *nido* clusters – molecular rearrangement – DFT – reaction pathway – ^{11}B NMR spectroscopy

■ INTRODUCTION

Mechanistic studies of the reactions of polyhedral boranes are quite rare and, therefore, the detailed mechanisms of their individual reactions are only beginning to be explored. The multiple possibilities for the reaction pathways have made such studies very difficult. This is also true for decaborane-like molecular shapes, where only experimental studies have been performed. Rearrangements of carbon vertices in the ten-vertex *nido*-5,6-$C_2B_8H_{12}$ (**1**) series were first observed in the base-induced racemisation[1] of (–)-*nido*-5,6-$C_2B_8H_{12}$ and conversion of the C-substituted 5-R-*nido*-5,6-$C_2B_8H_{11}$ (5-R-**1**) compounds (where R = Me, Ph) into their 6-R-*nido*-5,6-$C_2B_8H_{11}$ (6-R-**1**) counterparts.[2] The so-called double B-vertex swing (BVS) mechanism, shown in Scheme 1, was outlined without being computed to explain this rearrangement (hydrogen bridge positions omitted for clarity). It should be noted that other mechanisms have also been invoked to rationalize cluster rearrangements in the 10-vertex *nido* series, including vertex flips[3] and boron vertex extrusion and insertion.[4] In order to get a deeper insight into mechanistic studies of decaborane-based skeletons, we have performed computational studies of halogenated *nido*-5,6-$C_2B_8H_{12}$ in a concerted manner with experiments. The experiments serve to indicate the experimental uniqueness in terms of rearranging the skeleton with and acid and Lewis base as a reaction cycle.

Scheme 1 Representation of the double BVS mechanism (C = CH and the numbered cage positions stand for cluster BH units). BH units shown in gray indicate those involved in the flip, dotted lines indicate broken bonds.

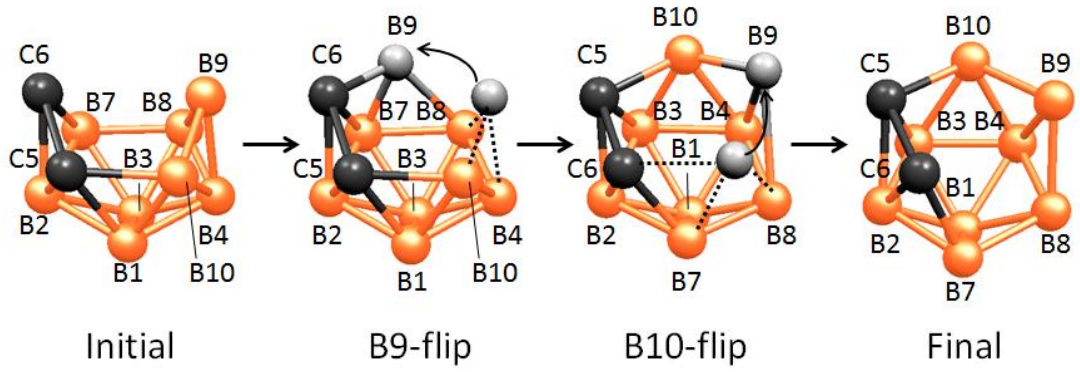

■ EXPERIMENTAL SECTION

Syntheses. The following synthetic procedures were used.

*Conversion of 7-X-nido-5,6-$C_2B_8H_{11}$ (7-X-**1**) (X = Cl, Br, I) compounds into the isomeric [10-X-nido-5,6-$C_2B_8H_{10}$]$^-$ anions (10-X-**1**$^-$).* A solution of 7-X-**1** (prepared according to ref. 5, see Figure 1; reaction scale 1 mmol) in hexane (15 ml) was treated with a solution of "proton sponge" (PS = 1,8-bis-dimethylaminonaphthalene, see Scheme S1) (reaction scale 1 mmol) in hexane (15 ml) at ambient temperature and the mixture was left standing for 6 h. The crystalline PSH^+[10-X-*nido*-5,6-$C_2B_8H_{10}$]$^-$ salts that precipitated quantitatively from the solution were isolated by filtration, and vacuum dried at room temperature for 4 h. Small samples (~20 mg) of these salts were analyzed by integrated NMR spectroscopy (for chemical shifts see Table 1) to indicate 75, 95, and 100% conversions to 10-X-substituted isomers (10-X-**1**$^-$) for X = Cl, Br, I, respectively.

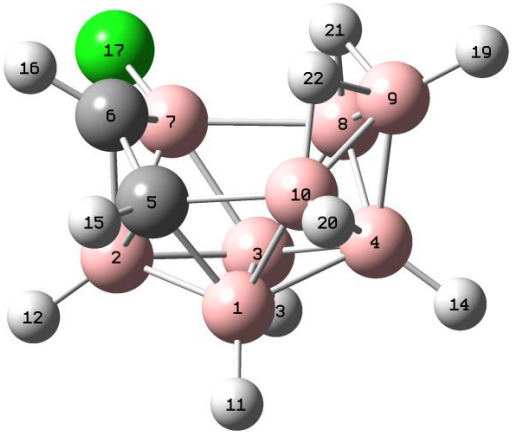

Figure 1 Geometric structure of 7-Cl-**1** together with atomic numbering, valid also for X = Br and I. 7-Cl-$\mathbf{1}^-$ has the same atomic numbering and its form, with the hydrogen bridge over B(8)–B(9), is computed to energetically favored by about 3.7 kcal mol^{-1} [B3LYP/6-31+G(d)] favored over the form where a hydrogen atom bridges B(9)–B(10). 10-X-**1** and 10-X-$\mathbf{1}^-$ would also use the same numbering.

*Direct conversion of 7-X-nido-5,6-$C_2B_8H_{11}$ (7-X-**1**) compounds (X = Cl, Br, I) to 10-X-nido-5,6-$C_2B_8H_{11}$ (10-X-**1**) isomers*. A solution of 7-X-**1**, prepared according to ref. 5, (reaction scale 1 mmol) in CH_2Cl_2 (15 ml) was treated with a solution of PS (reaction scale 1 mmol) in CH_2Cl_2 (15 ml) at ambient temperature and the mixture was left standing for 2 h. The mixture was then treated with concentrated H_2SO_4 (~5 ml, dropwise) under shaking and cooling at 0 °C. The organic layer was then separated and evaporated to dryness, which led to the isolation of a series of white crystalline compounds. These were identified by integrated NMR spectroscopy as the neutral 10-X-**1** isomers (for chemical shifts see Table 1) with conversions identical to those as in the preceding experiment.

*Conversion of 4-X-nido-5,6-$C_2B_8H_{11}$ (4-Cl-**1**) into the 3-X-nido-5,6-$C_2B_8H_{11}$ (3-X-**1**) isomer.* A solution of 4-Cl-**1**, prepared according to ref. 5, (40 mg, 0.25 mmol) in CH_2Cl_2 (5 ml) was treated with a solution of PS (64 mg, 0.3 mmol) in CH_2Cl_2 (5 ml) at ambient temperature and

the mixture was left standing for 2 h. The mixture was then treated with concentrated H_2SO_4 (~2ml, dropwise) under shaking and cooling at 0 °C. The organic layer was separated and evaporated to dryness, which led to the isolation of 3-X-**1** (66% conversion as assessed by integrated NMR spectroscopy). Pure 3-X-**1** can be obtained using liquid chromatography (LC), as in reference 5; for chemical shifts see Table 1. Note that according to electrophilic halogenation of the "bottom" part of **1** (ref. 5) only one monohalogeno derivative originated, 4-Cl-**1**, along with some dibromo and trichloro derivatives.

*Reconversion of 10-X-nido-5,6-$C_2B_8H_{11}$ (10-X-**1**) compounds (X = Cl, Br) to 7-X-nido-5,6-$C_2B_8H_{11}$ (7-X-**1**) isomers*. A solution of 10-X-**1** (X = Cl, Br; reaction scale 0.5 mmol) in CH_2Cl_2 was passed through a short silica gel column (~2.5 × 10 cm). Evaporation of the solvent from the eluate led to practically quantitative isolation of white crystalline compounds, which were identified by ^{11}B NMR spectroscopy as pure isomers 7-Cl-**1** and 7-Br-**1**.[1]

Computational details. Reaction pathway calculations and the corresponding molecular geometries, which were also used for magnetic properties calculations, were performed using Gaussian 09 software;[6] Amsterdam Density Functional (ADF) code[7] was used for the calculations of the shielding tensors.

Reaction pathway. The reaction pathway was computed at the B3LYP/6-31+G(d) level, as is common for this class of compounds. Single-point energy calculations were made at the B3LYP/6-311+G (2df,p) level and solvation effects of dichloromethane were computed at the SMD level[8] (including default SMD radii and non-electrostatic terms). Employing diffuse functions is justified since an anion is being studied. Unscaled zero-point energies, integrated heat capacities, and entropies were used to compute gas-phase free energies at 298 K. Free energies at 298 K in dichloromethane were calculated using eq 1.

$$\Delta G_{(\mathrm{sol,\ 298\ K})} = \Delta G_{(\mathrm{g,\ 298\ K})} + \Delta G_{(\mathrm{solv})} \qquad (1)$$

The transition vectors of all transition states were animated using the Molden[9] visualization code to verify that the motions were appropriate for converting reactant to product. In addition to that, intrinsic reaction coordinates (IRC) were constructed from each transition state to verify the corresponding reactant and product.

NMR computations. Calculations of shielding tensors with gauge-including atomic orbitals (GIAO) were performed at the MP2 level using IGLO-II all-electron basis sets[10] for H, B, and C. In contrast, for Br and I the quasirelativistic energy-consistent pseudopotential (ECP)[11] was used along with DZP basis sets, for details see Table S31. Molecular geometries for this purpose were optimized at the MP2/6-311++G(d,p) level, with Br and I being treated in the same manner as in the geometry optimizations. The ADF calculations utilized the BP86 functional and the same geometries as for the GIAO calculations. The two-component relativistic zeroth-order regular approximation (ZORA) method[12] including scalar and spin-orbit (SO)[13] corrections was employed for these computations; the all-electron triple-zeta basis set plus one polarization function (denoted TZP; from the ADF library) was used for all atoms. Magnetic shieldings were converted into relative ^{11}B chemical shifts using ^{11}B NMR of B_2H_6 as the primary reference.[14]

■ RESULTS AND DISCUSSION

Syntheses. Scheme 2 shows an interesting rearrangement cycle involving rearrangements of the previously reported[14] 7-X-substituted (where X = Cl, Br, I) derivatives of dicarborane (**1**), which are denoted 7-X-5,6-$C_2B_8H_{11}$ (7-X-**1**). Note that **1** exists as a racemic mixture from which its levorotary enantiomer was obtained by reacting the mixture with (+)-*N*-methylcamphidine.[1] In this context we opted for studying the rearrangement mechanism

instead of isolating an optically active form of 7-X-**1**. Deprotonation of 7-X-**1** compounds with one equivalent of PS in hexane or CH_2Cl_2 at ambient temperature led to a straightforward cluster rearrangement under the formation of a series of PSH^+ salts of the $[10\text{-X-}5,6\text{-}C_2B_8H_{10}]^-$ anion (10-X-**1**$^-$). Acidification of these salts with concentrated H_2SO_4 in CH_2Cl_2 generates a series of neutral carboranes 10-X-5,6-$C_2B_8H_{11}$ (10-X-**1**) with overall 7-X → 10-X conversions of 75, 95, and 100% for X = Cl, Br, I, respectively. It becomes obvious now that the observed 7-X-**1** → 10-X-**1** conversion cannot be expained by the BSV mechanism of Scheme 1 and therefore a new mechanism was designed. Moreover, the observed 4-Cl-**1** → 3-Cl-**1** conversion had not previously been tackled computationally and, therefore, the corresponding mechanism was explored, too.

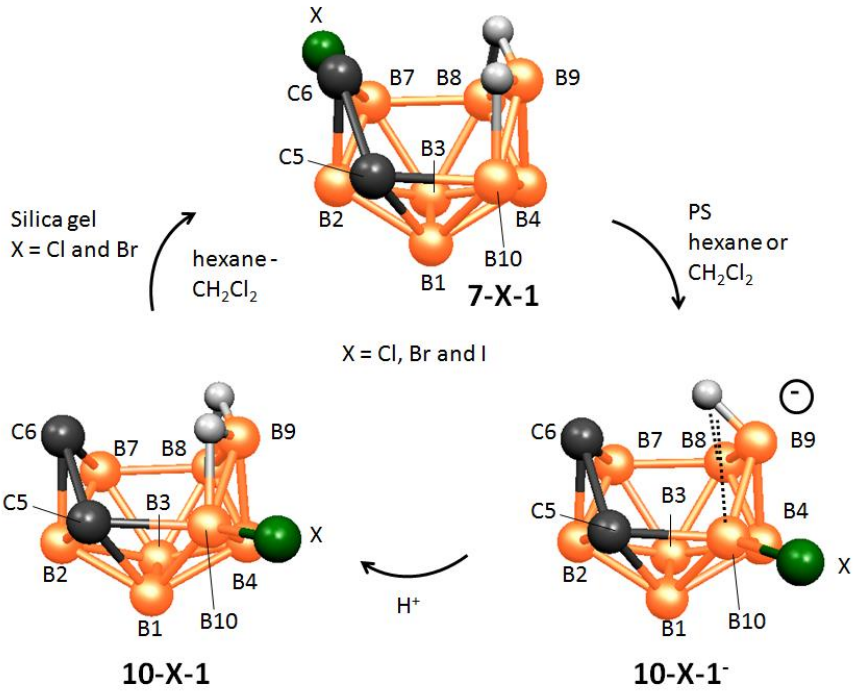

Scheme 2 Base-induced 7 → 10 rearrangement of halogenated derivatives of *nido*-5,6-$C_2B_8H_{12}$ (**1**). Note that the rearrangement of the B–X unit proceeds in the deprotonation step.

Another interesting, though difficult to rationalize, aspect is that the neutral chlorinated and brominated derivatives, 10-Cl-**1** and 10-Br-**1**, reconvert quantitatively to the original 7-Cl-**1**

and 7-Br-**1** compounds on passing through a silica gel column in CH_2Cl_2, while the iodinated counterpart, 10-I-**1**, remains unchanged under the same conditions. Derivatives 10-Cl-**1** and 10-Br-**1** must, therefore, be isolated with care using fractional vacuum sublimation at *ca.* 80 °C (bath) or crystallization from hexane at lower temperatures.

A similar rearrangement procedure (treatment with PS, followed by protonation) was also tested for the 4-chloroderivative 4-Cl-**1**[5] which another single monosubstituted derivative of **1**. This procedure led to an approximately 2:1 mixture of derivatives 3-Cl-**1** and 4-Cl-**1** (~66% conversion to 3-X-**1**). The 3-Cl and 4-Cl substituted derivatives are, therefore, interconvertible via a base-induced rearrangement process. The neutral 3-Cl-**1** and 4-X-**1** compounds obtained from the rearrangement reactions were separated by LC chromatography as reported earlier and characterized by NMR spectroscopy.[8] The as-yet unreported NMR data of their anionic counterparts (3-Cl-**1**$^-$ and 4-Cl-**1**$^-$) were estimated from those of their ~2:1 mixtures obtained from deprotonation reactions.

NMR spectroscopy. Once isolated 10-X-**1**$^-$ and 10-X-**1** derivatives were characterized using ^{1}H and ^{11}B NMR spectroscopy, and the use of [^{11}B-^{11}B]-COSY[15] techniques led to complete assignments of all boron resonances to individual cage BH units. (For ^{1}H and ^{11}B NMR shifts of individual derivatives see Table 1.)

Table 1 ^{11}B and ^{1}H NMR data for halogen derivatives of *nido*-[5,6-$C_2B_8H_{11}$]$^-$ (**1**$^-$) and 5,6-$C_2B_8H_{12}$ (**1**).

	δ(^{11}B) / ^{1}J(BH)[a]								δ(^{1}H)[b]		
Compound	B1	B7	B8	B3	B9	B10	B2	B4	CH6	CH5	μH
3-Cl-**1**$^-$[f]	–0.1	7.2	–6.2	–1.8 [c]	14.1[d]	–12.7	–33.4 / 168	–31.2 / 140	5.18	4.19	-3.00
GIAO[g]	1.5	7.6	–3.7	0.8	13.1	–10.4	–31.4	–27.5			
ZORA[h]	–4.4	3.6	–9.9	–2.4	10.2	–14.6	–36.4	–31.7			
4-Cl-**1**$^-$[f]	0.2	5.7	–6.2	–14.5	15.5[d]	–10.2	–33.4	–18.8	4.56	3.74	-3.18
GIAO[g]	–2.5	8.1	–2.0	–11.6	18.5	–12.9	–32.0	–10.6			
ZORA[h]	–8.6	3.9	–8.4	–16.8	15.2	–17.2	–36.6	–14.7			
10-Cl-**1**$^-$	–0.4 / 140	6.3 / 125	–5.7 / ~130	–14.1 / ~130	10.4[d]	–3.7[c]	–32.1 / 165	–28.9 / 140	4.98	3.69	–3.80
GIAO[g]	1.2	6.2	–7.3	–12.1	13.2	–0.1	–32.5	–26.4			
ZORA[h]	–5.2	2.3	–13.3	–17.0	10.5	–4.7	–37.5	–30.4			
10-Br-**1**$^-$	–0.1 / 136	7.5 / 122	–4.6 / 129	–13.5 / 134	12.8[d]	–9.2[c]	–31.3 / 168	–27.5 / 136	4.93	3.76	–3.84
GIAO[g]	0.6	6.8	–5.7	–12.4	15.5	–11.0	–32.5	–26.2			
ZORA[h]	–5.2	2.4	–12.2	–17.0	12.8	–12.3	–37.5	–30.0			
10-I-**1**$^-$	1.0 / 150	8.8 / 140	–2.1 / 140	–12.7 / 131	16.7[d]	–20.9 / 70[e]	–30.2 / 164	–26.1 / 140	4.87	3.97	–3.69
GIAO[g]	1.8	7.7	–4.5	–11.7	17.0	–4.5	–31.2	–25.0			
ZORA[h]	–4.6	3.5	–9.8	–16.7	15.0	–21.8	–36.1	–29.6			
10-Cl-**1**	7.3 / ~160	5.4 / ~145	–0.3 / ~145	–0.3 / ~145	–6.8 / 171	–1.8[c]	–27.1 / 174	–38.1 / 156	6.72	4.95	–2.03
GIAO[g]	7.7	6.7	–2.5	0.6	–7.6	3.2	–27.2	–37.7			
ZORA[h]	2.1	3.1	–7.3	-3.8	–13.3	–2.2	–32.0	–42.4			
10-Br-**1**	7.8 / ~170	6.8 / ~150	–0.4	–0.4	–5.3 / 168	–7.3 / 54[e]	–26.3 / 183	–37.4 / 159	7.20	5.04	–1.96
GIAO[g]	8.4	7.3	–0.4	0.7	–6.3	–3.6	–26.1	–36.8			
ZORA[h]	3.2	3.2	–5.5	–3.4	–11.6	–8.6	–31.0	–41.2			
10-I-**1**	8.7 / ~160	7.1 / 161	2.7 / 156	–0.6 / 149	–2.8 / 180	–23.2 / 54[e]	–25.4	–36.5 / 159	6.64	5.15	–0.56 / –1.84
GIAO[g]	9.5	7.5	1.8	0.6	–4.0	0.6	–25.0	–35.6			
ZORA[h]	4.4	3.5	–2.0	–3.8	–8.7	–23.1	–29.5	-40.4			

[a] Measured in $CDCl_3$, in ppm relative to $BF_3{\cdot}OEt_2$, assignments by {^{11}B-^{11}B}-COSY, ^{1}J(BH) in Hz (sometimes undefined due to signal overlap). [b] In ppm relative to TMS. [c] Singlet due to the substituted B-position. [d] Broad singlet. [e] Secondary doublet ^{11}B-μ$H_{9,10}$ splitting.[f] Assigned from the mixture of 3-Cl and 4-Cl substituted derivatives. [g] Nonrelativistic GIAO-MP2/II//MP2/6-311++G**, for Br and I ECP+DZP was used (see computational details). [h] Relativistic ZORA-BP86/TZ2P//the same geometries as in GIAO computations.

Inspection of Table 1 shows that the ^{11}B NMR spectra of all derivatives of **1** isolated in this study consist of eight different boron resonances, of which one shows as a singlet due to the substituted boron vertex (B10, B3 or B4). ^{1}H NMR spectra indicate two different CH resonances, together with broad high-field hydrogen bridge resonances. The intensities of the hydrogen-bridge resonances indicate whether there is one bridging hydrogen atom (anionic species) or two bridging hydrogen atoms (neutral compounds). The ^{11}B NMR spectra are similar to those of the parent dicarboranes **1** and **1**$^{-}$ except that the singlets for the substituted boron atoms exhibit enhanced deshielding properties, a phenomenon generally known for α-shifts of halogenated boron clusters.[5] The deshielding increases in the series X = Cl > Br > I. Inspection of Table 1 and α shifts in reference 5 also suggests that deshielding by chlorine substituted into different vertices of **1** decreases remarkably in the order B4 > B3 > B7 > B10, in agreement with decreasing negative charge.[16]

Table 1 shows a very good agreement between the GIAO-MP2/II-computed and experimental ^{11}B chemical shifts for all eight compounds, apart from those boron atoms that are bonded to bromine and iodine substituents, with the disagreement more pronounced for iodine. Since inclusion of spin-free relativistic effects by pseudopotentials in the GIAO calculations does not solve the problem, these discrepancies at this level may be seen as an indicator of the need for an appropriate level of theory that takes into account relativistic spin-orbit effect[17] on the chemical shifts. Such effects are known to overcompensate the trends caused by decreasing electronegativity for the heavier halogen substituents.[18] Indeed, employing the two-component relativistic zeroth-order regular approximation (ZORA) method within the ADF code in order to account for the spin-orbit corrections (SO) to the ^{11}B shifts in the corresponding B(10) improves the fit between the theory and experiment for this atom considerably, as shown in Table 1. The largest SO correction was found

computationally for B(10) in 10-I-**1**, reaching almost 22 ppm at the ADF level used. ADF results are systematically shielded to lower frequencies. The B(10) atom is exceptional in this respect, due to the above-mentioned spin-orbit coupling. For example, the ^{11}B NMR chemical shift for B(10) computed at ADF level in 10-Br-**1**$^-$ without such a contribution would have been computed at even lower frequency than –12.3 ppm. The SO contribution to the overall shielding tensor of 6.3 ppm compensates such a trend. The effect of SO coupling on correctly computed ^{11}B NMR chemical shifts can be even more pronounced. For example, in BBr_3 and BI_3 GIAO computations with the same model chemistry cause $\delta(^{11}B)$ NMR to be 73.1 and 102.8 ppm, whereas the measured value are 38.7 and –7.9 ppm, respectively. Inclusion of SO coupling within the ADF scheme improves the fit considerably, *viz.* 38.3 and –0.1 ppm, respectively. The same trend is observed for BBr_4^- and BI_4^-: GIAO 15.6 and 25.0 ppm, respectively; experimental –23.8 and –127.5 ppm, respectively; ADF –27.2 and –108.6 ppm, respectively.[19]

Computed ^{11}B NMR chemical shifts using the GIAO-MP2/II approach with the basis sets used (see Computational details) show very good agreement with the experimental values, which justifies our assumption that the geometries of all eight NMR-computed compounds (six 10-X-derivatives are newly prepared) with a halogen atom bonded to B(10) are very good representation of their molecular geometries in solution, with SO contributions playing significant roles when making such a comparison for all four Br and I derivatives. Tables S1–S8 provide the corresponding atomic coordinates.

Figure 2 shows that the plot of chemical shift changes ($\Delta\alpha$) at the substituted site, where $\Delta\alpha = \delta_s - \delta_p$, and subscripts s and p relate to the substituted and parent compound. For the isolated derivatives 10-X-**1** versus the same characteristics for 7-X-**1**[5] (X = Cl, Br, I) derivatives the plot is linear, which indicates that the character of halogen shielding in the ten-vertex *nido* series of boron-cluster compounds is similar to that in the 7-vertex series.

(For a similar correlation of the chemical shifts for 7-X-**1** with those for 5-X-$B_{10}H_{13}$ compounds, see reference 5.) A similar linearity would also be expected for other isomers if the corresponding derivatives were available. As demonstrated by graphical inter-comparison in Figure S1, the reported ^{11}B NMR spectra are similar to those of the parent dicarbaboranes **1** and **1**$^{-}$.

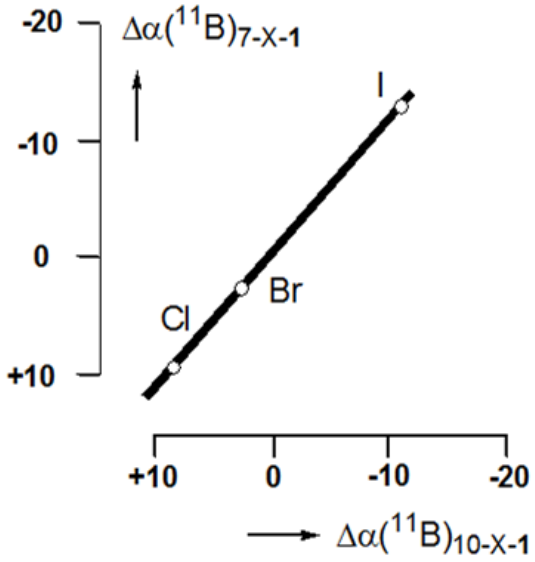

Figure 2 Plot showing the linear relationship between Δα(^{11}B) halogen shifts for 10-X-*nido*-5,6-$C_2B_8H_{11}$ (10-X-**1**) and 7-X-*nido*-5,6-$C_2B_8H_{11}$ (7-X-**1**) derivatives (X = Cl, Br, I) reflecting similar shielding behavior within the ten-vertex *nido* dicarbaborane series (data for 7-X-**1** compounds from reference 5).

Proposed reaction pathways. The isomerization of the 10-vertex *nido*-5,6-dicarbaborane framework was studied using hybrid-functional B3LYP within the DFT scheme (see Figures 3 and 4, and 5 and 6). We have recently found that DFT and MP2 model chemistries are quite consistent in terms of individual computed barries and, therefore, we opted for a less CPU-demanding DFT scheme to examine the reaction profile that is being studied.[20] Employing diffuse functions is important because an anionic species is considered. The initial deprotonation step of 7-Cl-**1** by PS is spontaneous by –3.4 kcal mol^{-1}, whereas this kind of deprotonation is about 1.6 kcal mol^{-1} less spontaneous for 4-Cl-**1** (eq 2).

$$7(4)\text{-Cl-}5,6\text{-}C_2B_8H_{11} + PS \rightarrow 7(4)\text{-Cl-}5,6\text{-}C_2B_8H_{10}^- + PSH^+ \quad (2)$$

However, the PS is unable to remove a second proton as indicated by nonspontaneous free energy changes of 29.7 and 29.9 kcal mol^{-1} for the 7- and 4-isomers, respectively, according to eq 3.

$$7(4)\text{-Cl-}5,6\text{-}C_2B_8H_{10}^- + PS \rightarrow 7(4)\text{-Cl-}5,6\text{-}C_2B_8H_9^{2-} + PSH^+ \quad (3)$$

We also determined the free energy change for removing a chloride anion from 7-Cl-**1**$^-$ as well as from 4-Cl-**1**$^-$ to form neutral $C_2B_8H_{12}$. The large calculated values of 37.2 kcal mol^{-1} and 37.8 kcal mol^{-1}, respectively indicate that rearrangements on the neutral 5,6-$C_2B_8H_{12}$ PES is not likely, which is supported by the experiments. Therefore, we believe the most likely species involved in the rearrangements are the 7-Cl-**1**$^-$ and 4-Cl-**1**$^-$ anions.

There are three possible pathways of the 7-Cl-**1**$^-$ to 10-Cl-**1**$^-$ rearrangement, with solvation effects included, suggested by the computations. They proceed through a series of six, five, and eight transition states (TS), respectively. Some TSs of the last reaction option can be related to very energetically demanding diamond-square-diamond-based (DSD) rearrangement[21] and bridge-terminal-bridge migrations. Since the initial barrier is computed to be quite high (46 kcal mol^{-1}, see Figures S2 and S3) we will not consider such a pathway further. Although the second mechanistic alternative is energetically more favorable (a series of bridge-terminal-bridge migrations), see Figures S4 and S5, than the latter, we opted for reporting the next computed pathway as justified by indirect experimental evidence. Hence, such a rearrangement is likely to proceed through formation of [Cl$^-$-1,2-*closo*-$C_2B_8H_{10}$] as one of the intermediates. However, this intermediate is computed to be more stable than 7-Cl-

1^{-}, which might be the consequence of model chemistry and basis set chosen. Moreover, implicit solvation methods, such as SMD, are sometimes poor at calculating the solvation free energies of single-atom ions, such as Cl^{-}. Its energy in dichloromethane is computed to be –60.6 kcal mol^{-1} at B3LYP/6-311+G(2df,p),[22] which is "too negative". Consequently, the uncertainty in the solvation-free energy of the [Cl^{-}-1,2-*closo*-$C_2B_8H_{10}$] complex may be larger than for the other stationary points. It was found very recently that attacking **1**$^{-}$ with $N^{+}H(C_2H_5)_4$ results in the formation of *closo*-$C_2B_8H_{10}$.[23] The transition state of the latter dehydrogenation process, from which the parent *closo* arrangement originates, bears a strong resemblence with TS2 of the 7-Cl-**1**$^{-}$ *vs.* 10-Cl-**1**$^{-}$ rearrangement. On the basis of this experimental support, we report here the mechanism that includes the above *closo*-ten-vertex complex as the most probable one. It is also favorable energetically since it is the lowest free energy pathway that we could find. Figure 3 illustrates this mechanistic design, whilst Figure 4 illustrates the energetic balance of this reaction pathway, the final product G being drawn in two ways.

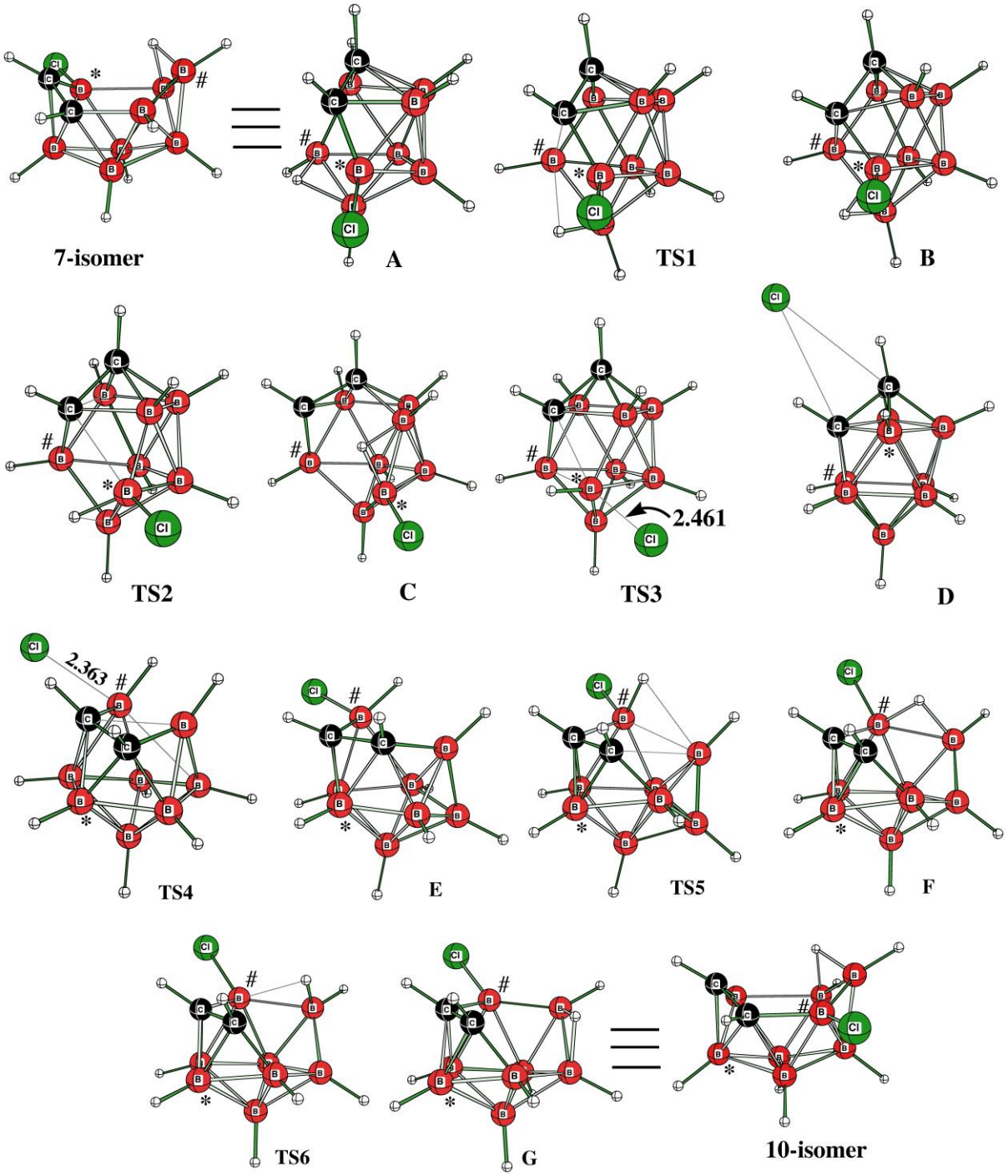

Figure 3 The individual stationary points during the 7-Cl-**1**$^{-}$ *vs.* 10-Cl-**1**$^{-}$ rearrangement as suggested by the most experiment-verifying computations. Boron atoms marked with a * symbol start in the reactant as B7 while boron atoms marked with a # end up as B10 in the product. For the model chemistries used see Computational details.

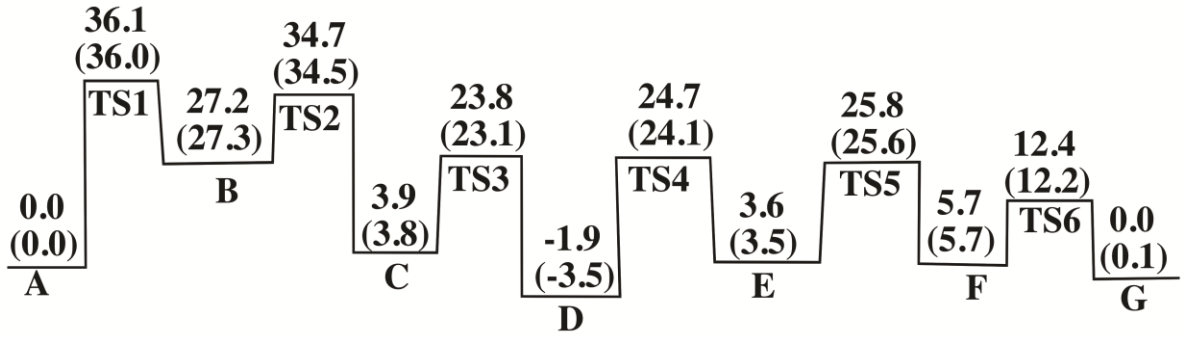

Figure 4 Reaction enthalpies (free energies) for the 7-X-**1**$^{-}$ *vs.* 10-X-**1**$^{-}$ rearrangement at 298 K in kcal mol^{-1}. For free energies see also eq 1. SMD (dichloromethane) was used considering solvation effects at B3LYP/6-311+G(2df,p)//B3LYP/6-31+G(d).

The 4-Cl-**1**$^{-}$ *vs.* 3-Cl-**1**$^{-}$ rearrangement is based on simple bridge-terminal-bridge hydrogen migrations and DSD steps as shown in Figure 5, in which the final product E is also drawn in two ways. Figure 6 provides the energetic profile with this second reaction process taken into consideration. The 4-isomers convert to intermediate D, from which four different pathways are possible. Two pathways go to the 3-isomer and two pathways go to the 8-isomer. The most favorable pathway is one of the two that provides the 3-isomer. Since there is no experimental availability of the 8-isomer, the interplay between the theory and experiment is impossible to study for this material.

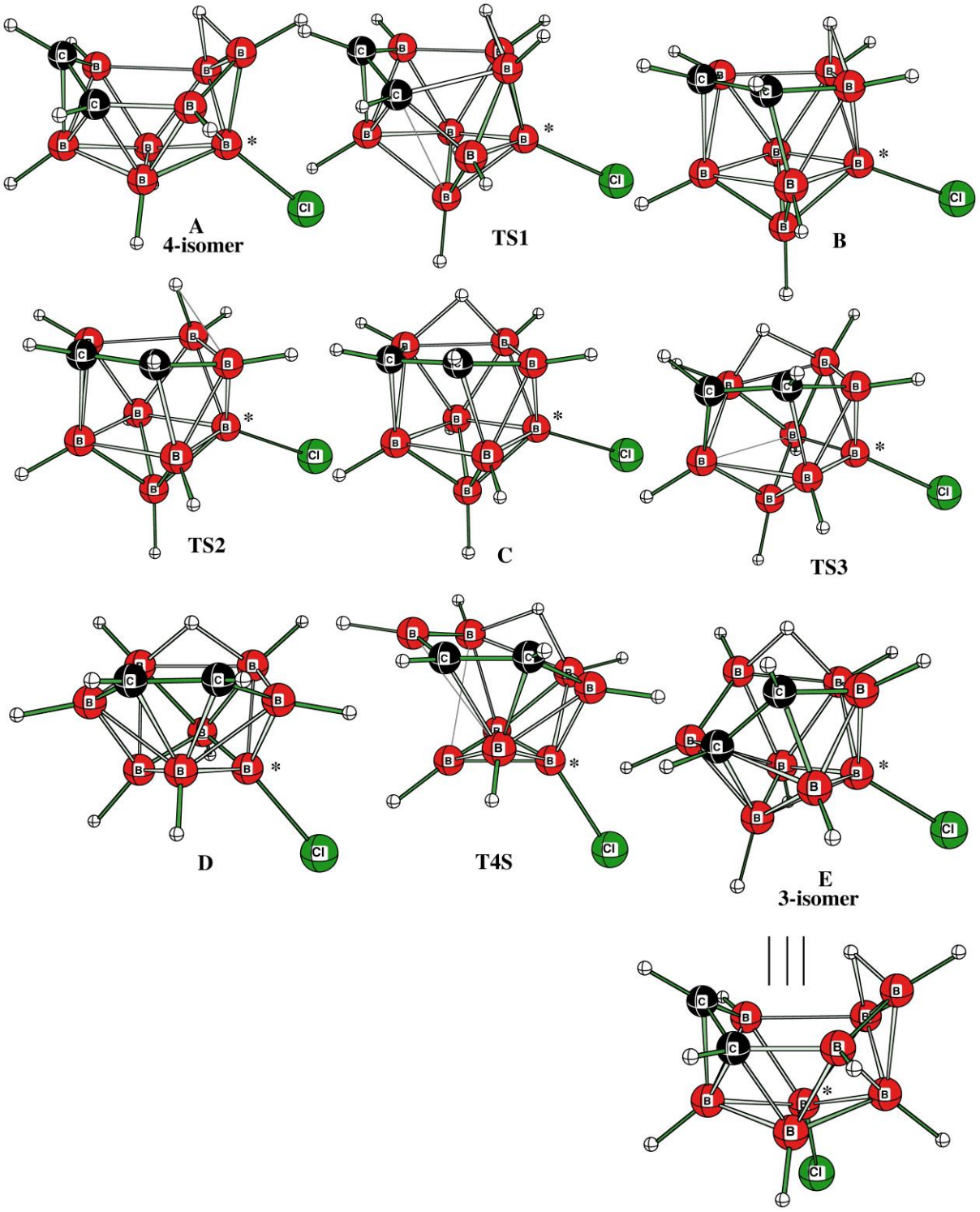

Figure 5 The individual stationary points during the 4-Cl-**1**$^-$ *vs.* 3-Cl-**1**$^-$ rearrangement as suggested by the most experiment-verifying computations. The boron atoms marked with * start the mechanism as B4 and end as B3. For the model chemistries used see Computational details.

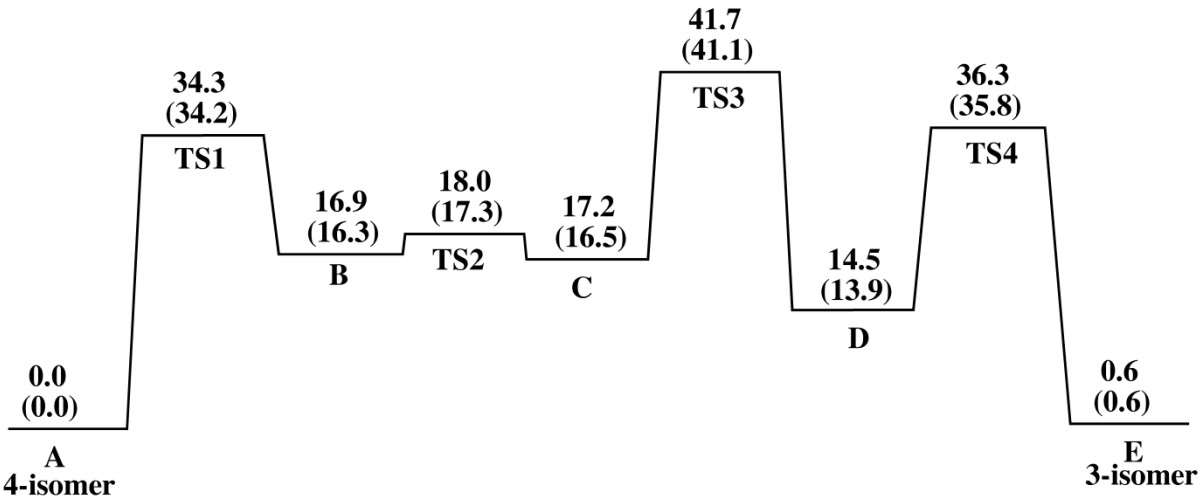

Figure 6 Reaction enthalpies (free energies) for the 4-Cl-**1**$^-$ *vs.* 3-Cl-**1**$^-$ rearrangement at 298 K in kcal mol^{-1} . For free energies see also eq 1. SMD (dichloromethane) was used considering solvation effects at B3LYP/6-311+G(2df,p)//B3LYP/6-31+G(d).

Armed with Ref. 23a, we also explored the Cl–B bond-breaking transition state, TS, as shown in Figure 7 that might result in the [Cl$^-$-1,2-*closo*-$C_2B_8H_{10}$] complex, identified as intermediate D during the 7-Cl-**1**$^-$ *vs.* 10-Cl-**1**$^-$ rearrangement. Indeed, IRC computations did show that the intermediate that followed from TS is the same as intermediate D from which both the 7-isomer and 10-isomers are affordable (see Figures 3 and 4). Attempts to prove the existence of such a complex by adding (CH_3COO)Ag to **1** in the presence of PS failed, since no AgCl was observed. Conceivably, reductive and oxidative properties of the boron hydride and Ag^+, respectively supressed the simple cation/anion exchange. The barrier from the 4-isomer to TS is only a little higher in free energy than the others mentioned. Note also that the 4-isomer is 1.6 kcal mol^{-1} less stable than the 7-isomer at SMD/B3LYP/6-311+G(2df,p)//B3LYP/6-31+G(d). To sum up, we have pathways connecting the 3-, 4-, 7-, and 10-isomers when the initial barrier for the 4-Cl-**1**$^-$ *vs.* 3-Cl-**1**$^-$ rearrangement is

considered to be that provided in Fig. 7. Similar unprecedent rearrangements have recently been also studied.[23d]

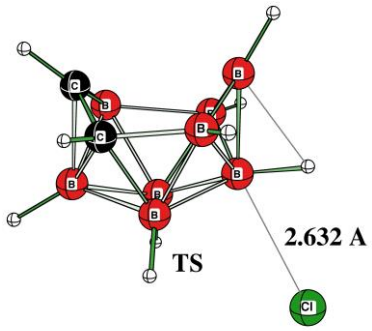

Figure 7 The Cl–B bond-breaking transition state (TS) depicted is computed to lie 48.6 (46.9) kcal mol^{-1} above the 4-isomer computed at B3LYP/6-311+G(2df,p)//B3LYP/6-31+G(d). SMD (dichloromethane) was used considering solvation effects at B3LYP/6-311+G(2df,p)//B3LYP/6-31+G(d).

The computed sums of the individual free energy barriers for both processes are somewhat higher than expected from the experimental condition present during rearrangements, which might be mainly attributed to anionic character of 7-Cl-**1**$^{-}$ and 4-Cl-**1**$^{-}$. Note that such high barriers are computed even for neutral systems that undergo reactions under modest conditions.[24]

The Cartesian coordinates of all 13 stationary points for the first process and 9 stationary points for the second process are given in Supporting Information and, in the case of transition states, individual imaginary frequencies are also provided.

■ CONCLUSIONS

Reactions of boron hydrides can involve many competing pathways and intermediates with femtosecond lifetimes, which is in huge contrast to well-understood organic chemistry. Hence, reaction mechanisms can be very complex because there is often little energy

difference between various intermediates and transition states.[25] Indeed, we have now found that the earlier suggested BVS mechanism totally differs from that reported here when applied to base-induced rearrangements of halogen substituted derivatives of **1**. The following conclusions can be drawn: the 7-X derivatives of carborane **1** (where X = Cl, Br, I) undergo (on deprotonation and re-protonation) a complete rearrangement of all cluster positions to form carboranes 10-X-5,6-$C_2B_8H_{11}$ (10-X-**1**). The same applies to the 4-Cl derivative of carborane **1**, whose rearrangements give 3-X-5,6-$C_2B_8H_{11}$ (3-Cl-**1**). Experiments indicate that thermodynamic stabilities of individual derivatives of **1** are quite different. For example, the stabilities of 10-X-**1** compounds decrease in the order I > Br > Cl, while the reverse order Cl > Br > I seems to apply for the 7-X-**1** series. On the other hand, the stabilities of 3-Cl-**1** and 4-Cl-**1** derivatives appear to be comparable. Computations also show that the [Cl^--1,2-*closo*-$C_2B_8H_{10}$] complex, in the form of an intermediate, is common for both rearrangements.

Positively charged outer surfaces of bromine and, to a large extent, of iodine (σ-holes) result in long-range interactions with negatively charged hydrogens in all transition states of the 7-X-$\mathbf{1}^-$ *vs.* 10-X-$\mathbf{1}^-$ rearrangement, which leads to their stabilization and, consequently, to lower barriers in the corresponding reaction profiles than in the case of chlorine. This may offer an explanation of the increasing yields on going from chlorine to iodine.[26] We also note that, from a geometrical point of view, a direct exchange of Cl bound to B(7) with H bound to B(10) is impossible since the separation of such Cl and H atoms is computed to be 625 pm at B3LYP/6-31+G(d) as revealed from the reaction profile for **A** in Figure 4. Note that this distance is 616 pm when calculated using MP2/6-311++G(2df,p). This observation further supports our decision to use a DFT computational protocol for exploring the reaction profile. The same holds for the 4-Cl-$\mathbf{1}^-$ isomer, where the corresponding distance is computed to be about half of the above values. Experiments aimed at the isolation of the still unknown

derivatives of **1** substituted in positions other than 3, 4, 7 and 10 are in progress, as well as in other clusters with hexagonal boat-like shape.

■ ASSOCIATED CONTENT

Supporting Information

Scheme S1 shows protonized proton sponge, Figures S2-S5 illustrate another two reaction possibilities. Calculated atomic coordinates for all eight calculated structures are in Tables S1–S8. Calculated atomic coordinates for all 13 stationary point from the first rearrangement process, and all 9 stationary points from the second process are in Tables S9–S30. Table S31 provides details of the model chemistries used for Br and I.

■ ACKNOWLEDGMENTS

The work was supported by the Czech Science Foundation (project no. 16-01618S). The Alabama Supercomputer Center is thanked for a generous allocation of computer time. We thank the EPSRC for funding a Fellowship for D.A.W. (EP/I004122). This work has made use of the resources provided by the EPSRC UK National Service for Computational Chemistry Software (NSCCS) at Imperial College London.

Funding

All data created using EPSRC funding are available by request from the University of York Data Catalogue http://dx.doi.org/10.15124/959c9a82-79d5-42db-95eb-4d53852ddc37.

Notes

The authors declare no competing financial interest.

■ REFERENCES

1. Štíbr, B.; Plešek, J.; Zobáčová, A. Optically-Active (-)-5,6-Dicarba-*nido*-Decaborane(12). Polyhedron **1982**,1, 824 - 826.

2. (a) Štíbr, B.; Holub, J.; Jelínek, T.; Grüner, B.; Fusek, J.; Plzák, Z.; Teixidor, F.; Viňas C.; Kennedy, J. D. A Return to the Plesek Reaction and Some Useful Variations. Carbon-Substituted Methyl and Phenyl Derivatives of 5,6-Dicarba-*nido*-decaborane(12), *nido*-5,6-$C_2B_8H_{12}$. *Collect. Czech. Chem. Commun.* **1997**, *62*, 1229 - 1238; (b) Janoušek, Z.; Kaszynski, P.; Kennedy, J. D.; Štíbr, B. NMR Assignments of [6-R-*nido*-5,6-$C_2B_8H_{10}$]$^-$ Anions (where R = H, Me, and n-C_6H_{13}). An Irreversible 5 → 6 Alkyl Migration *via* a B9 Vertex-Swing Mechanism.*Collect. Czech. Chem. Commun.* **1999**, *64*, 986 - 992.

3. (a) Gaines, D. F; Lot, J. W. Manganese and Rhenium Metalloboranes Containing Tridentate Borane Ligands $B_9H_{13}^{2-}$ and $B_9H_{12}L^-$ (L = Tetrahydrofuran or Diethyl Ether). *Inorg. Chem.* **1974**, *13*, 2261 - 2267; (b) Bould, J.; Dorfler, U.; Thornton-Pett, M.; Kennedy, J. D. A Rearrangement of the 10-Boron *nido / arachno* Decaboranyl Cluster. *Inorg. Chem. Commun.* **2001**, *4*, 544 - 546; (c) Bown, M.; Fowkes, H.; Fontaine, X. L. R.; Greenwood, N.; Kennedy, J. D.; MacKinnon, P.; Nestor, K. Comparative Metallaborane Chemistry: Preparation and Nuclear Magnetic Resonance Studies of some *nido*-5-Metalladecaboranes of Rhodium, Iridium, Ruthenium, and Osmium. *J. Chem. Soc., Dalton Trans.* **1988**, 2597 - 2600.

4. Macias, R.; Bould, J.; Holub, J.; Štíbr, B.; Kennedy, J. D. Ten-Vertex Polyhedral Azametallaborane Chemistry: a Unique *nido*-6,9 to *nido*-6,8-Cluster Isomerization. *Dalton Trans*. **2008**, 4776 - 4783.

5. Holub, J.; Bakardjiev, M.; Štíbr, B. Electrophilic Halogenation of *nido*-5,6-$C_2B_8H_{12}$. *Collect. Czech. Chem. Commun.* **2006**, *71*, 1549 - 1556.

6. Frisch, M. J.; Trucks, G. W.; Schlegel, H. B.; Scuseria, G. E.; Robb, M. A.; Cheeseman, J. R.; Scalmani, G.; Barone, V.; Mennucci, B.; Petersson, G. A.; Nakatsuji, H.; Caricato, M.; Li, X.; Hratchian, H. P.; Izmaylov, A. F.; Bloino, J.; Zheng, G.; Sonnenberg, J. L.; Hada, M.; Ehara, M.; Toyota, K.; Fukuda, R.; Hasegawa, J.; Ishida, M.; Nakajima, T.; Honda, Y.; Kitao, O.; Nakai, H.; Vreven, T.; Montgomery, Jr., J. A.; Peralta, J. E.; Ogliaro, F.; Bearpark, M.; Heyd, J. J.; Brothers, E.; Kudin, K. N.; Staroverov, V. N.; Kobayashi, R.; Normand, J.; Raghavachari, K.; Rendell, A.; Burant, J. C.; Iyengar, S. S.; Tomasi, J.; Cossi, M.; Rega, N.; Millam, J. M.; Klene, M.; Knox, J. E.; Cross, J. B.; Bakken, V.; Adamo, C.; Jaramillo, J.; Gomperts, R.; Stratmann, R. E.; Yazyev, O.; Austin, A. J.; Cammi, R.; Pomelli, C.; Ochterski, J. W.; Martin, R. L.; Morokuma, K.; Zakrzewski, V. G.; Voth, G. A.; Salvador, P.; Dannenberg, J. J.; Dapprich, S.; Daniels, A. D.; Farkas, Ö.; Foresman, J. B.; Ortiz, J. V.; Cioslowski, J.; Fox, D. J. *Gaussian 09, Revision D.1*, Gaussian, Inc., Wallingford CT, 2009.

7. (a) te Velde, G.; Bickelhaupt, F. M.; Baerends, E. J.; Fonseca Guerra, C.; van Gisbergen, S. J. A.; Snijders, J. G.; Ziegler, T. Chemistry with ADF. *J. Comput. Chem.* **2001**, *22*, 931 - 967; (b) Baerends, E. J.; Autschbach, J.; Bérces, A.; Bo, C.; Boerrigter, P. M.; Cavallo, L.; Chong, D. P.; Deng, L.; Dickson, R. M.; Ellis, D. E.; Fan, L.; Fischer, T. H.; Fonseca Guerra, C.; van Gisbergen, S. J. A.; Groeneveld, J. A.; Gritsenko, O. V.; Grüning, M.; Harris, F. E.; van den Hoek, P.; Jacobsen, H.; van Kessel, G.; Kootstra, F.; van Lenthe, E.; McCormack, D. A.; Osinga, V. P.; Patchkovskii, S.; Philipsen, P. H. T; Post, D.; Pye, C. C.; Ravenek, W.; Ros, P.; Schipper, P. R. T.; Schreckenbach, G.; Snijders, J. G.; Sola, M.; Swart, M.; Swerhone, D.; te Velde, G.; Vernooijs, P.; Versluis, L.; Visser, O.; van Wezenbeek, E.; Wiesenekker, G.; Wolff, S. K.; Woo, T. K.; Ziegler, T. *ADF2004.01*, SCM, Theoretical Chemistry, Vrije Universiteit, Amsterdam, The Netherlands.

8. Marenich, A. V.; Cramer, C. J. ; Truhlar, D. G. Universal Solvation Model Based on Solute Electron Density and on a Continuum Model of the Solvent Defined by the Bulk Dielectric Constant and Atomic Surface Tensions. *J. Phys. Chem. B* **2009**, *113*, 6378 - 6396.

9. Schaftenaar, G.; Noordik, J. H. Molden: a Pre- and Post-processing Program for Molecular and Electronic Structures. *J. Comput.-Aided Mol. Design* **2000**, *14*, 123 - 134.

10. Kutzelnigg, W.; Fleischer, U.; Schindler, M. *The IGLO-Method: Ab Initio Calculation and Interpretation of NMR Chemical Shifts and Magnetic Susceptibilities*; Vol. 23; Springer-Verlag: Heidelberg, 1990.

11. Bergner, A.; Dolg, M., Küchle, W.; Stoll, H; Preuss, H. *Ab initio* Energy-adjusted Pseudopotentials for Elements of Groups 13–17. *Mol. Phys.* **1993**, *80*, 1431-1441.

12. (a) van Lenthe, E.; Baerends, E. J.; Snijders, J. G. Relativistic Total Energy Using Regular Approximations. *J. Chem. Phys.* **1994**, *101*, 9783; (b) van Lenthe, E.; van Leeuwen, R.; Baerends, E. J.; Snijders, J. G. Relativistic Regular Two-Component Hamiltonians. *Int. J. Quantum Chem.* **1996**, *57*, 281- 293; (c) van Lenthe, E.; Baerends, E. J.; Snijders, J. G. Relativistic Regular Two-Component Hamiltonians. *J. Chem. Phys.* **1993**, *99*, 4597.

13. van Lenthe, E.; Snijders, J. G.; Baerends, E. J. The Zero-Order Regular Approximation for Relativistic Effects: The Effect of Spin–Orbit Coupling in Closed Shell Molecules. *J. Chem. Phys.* **1996**, *105*, 6505.

14. Onak, T. P.; Landesman, H. L.; Williams, R. E.; Shapiro, I. The B^{11} Nuclear Magnetic Resonance Chemical Shifts and Spin Coupling Values for Various Compounds. *J. Phys. Chem.* **1959**, *63*, 1533 - 1535.

15. Hutton, W. C.; Venable, T. L.; Grimes, R. N. Two-dimensional Boron-11-Boron-11 Nuclear Magnetic Resonance Spectroscopy as a Probe of Polyhedral Structure: Application to Boron Hydrides, Carboranes, Metallaboranes, and Metallacarboranes. *J. Am. Chem. Soc.* **1984**, *106*, 29 – 37.

16. Štíbr, B.; Heřmánek, S.; Janoušek, Z.; Plzák, Z.; Dolanský, J.; Plešek, J. A ^{11}B NMR-Study of 5,6-Dicarba-*nido*-Decaborane(12). *Polyhedron* **1982**, *1*, 822-824.

17. Kaupp, M.; Malkina, O. L.; Malkin, V. G.; Pyykkö, P. How Do Spin–Orbit-Induced Heavy-Atom Effects on NMR Chemical Shifts Function? Validation of a Simple Analogy to Spin–Spin Coupling by Density Functional Theory (DFT) Calculations on Some Iodo Compounds. *Chem. Eur. J.* **1998**, *4*, 118 - 126.

18. Kidd, R. G. Nuclear Shielding of the Transition Metals. *Ann. Rep. NMR Spectrosc. A* **1980**, *10*, 1-79.

19. (a) Hnyk, D.; Macháček, J. XIIth International Congress of Quantum Chemistry, Kyoto, Japan, **2006**, C176; (b) a similar trend was observed for the isoelectronic series CX_4 (X = F, Cl, Br, I) in the corresponding ^{13}C spectra, see Mercier, H. P. A.; Moran, M. D.; Schrobilgen, Ch. S.; Suontamo R. J. The Syntheses of Carbocations by Use of the Noble-Gas Oxidant, [$XeOTeF_5$] [$Sb(OTeF_5)_6$]: The Syntheses and Characterization of the CX_3^+ (X= Cl, Br, $OTeF_5$) and $CBr(OTeF_5)_2^+$ Cations and Theoretical Studies of CX_3^+ and BX_3(X = F, Cl, Br, I, $OTeF_5$). *J. Am. Chem. Soc.* **2004**, *126*, 5533-5548 and references therein; (c) ^{31}P spectra are also consistent: Kaupp, M.; Aubauer, Ch.; Engelhardt, G.; Klapötke, T. M.; Malkina, O. L. The PI_4^+ Cation has an Extremely Large Negative ^{31}P Nuclear Magnetic Resonance Chemical Shift, Due to Spin–Orbit Coupling: A Quantum-Chemical Prediction and its Confirmation by Solid-State Nuclear Magnetic Resonance Spectroscopy. *J. Chem. Phys.* **1999**, *110*, 3897-3902.

20. Bakardjiev, M.; Holub, J.; Hnyk, D.; Štíbr, B.; Růžičková, Z.; Růžička, A. An Unexpected Rearrangement of Carbon Vertexes in the Tricarbollide Series. Asymmetrical 7-Aryl-*nido*-7,8,9-$C_3B_8H_{11}$. *J. Organomet. Chem.* **2016**, *805*, 117 - 121.

21. The diamond-square-diamond (DSD) mechanism first coined by Lipscomb (Lipscomb, W. N. Framework Rearrangement in Boranes and Carboranes. *Science* **1966**, *153*, 373 - 378) is one of the proposed mechanistic studies of polyhedral boranes and explains, for example, conversion of 1,2-*closo*-$C_2B_{10}H_{12}$ to 1,12-*closo*-$C_2B_{10}H_{12}$ *via* 1,7-*closo*-$C_2B_{10}H_{12}$, where two DSD-based transition states are needed for the entire conversion, the latter compound being regarded as an intermediate in this context. The barrier of the first step is computed to be quite high (62 kcal mol^{-1}); see, for example, Salinger, R. M.; Frye, C. L. Facile Polyhedral Rearrangement of Icosahedral Silylcarboranes. *Inorg. Chem.* **1965**, *4*, 1815 - 1816. The DSD rearrangements have been used to rationalize a number of isomerizations found in boranes and carboranes; for other examples see Wade, K. *In Electron Deficient Compounds*; Nelson: London, 1971. This processes proceeds through a cuboctahedron cage as also determined experimentally, see Hosmane, N. S.; Zhang H.; Maguire, J. A.; Wang, Y.; Thomas, C. J.; Gray T. G. The First Carborane with a Distorted Cuboctahedral Structure. *Angew. Chem. Int. Ed. Engl.* **1996**, *35*, 1000 - 1001.

22. Solvation free energy of Cl^- in 1,1-dichloroethane amounts to –56.9 kcal mol^{-1}, for its determination a one-layer continuum model was used, see: Abraham, M. H.; Liszi, J. Calculations on Ionic Solvation 1. Free-Energies of Solvation of Gaseous Univalent Ions Using a One-Layer Continuum Model. *J. Chem. Soc., Faraday Trans.* **1978**, *74*, 1604 - 1614.

23. a) Tok, O. L.; Bakardjiev, M.; Štíbr, B.; Hnyk, D.; Holub, J.; Padělková, D.; Růzička, A. Click Dehydrogenation of Carbon-Substituted *nido*-5,6-$C_2B_8H_{12}$ Carboranes: A General

Route to *closo*-1,2-$C_2B_8H_{10}$ Derivatives. *Inorg. Chem.* **2016**, *55*, 8839 - 8843.; b) Such a finding is supported by the earlier observed disproportionation of $\mathbf{1}^-$ and one of its product being 1,2-*closo*-$C_2B_8H_{10}$, see: Štíbr, B.; Plešek, J.; Heřmánek, S. *Collect. Czech. Chem. Commun.* **1973**, *38*, 338. c) **1** can be easily converted in a one-pot reaction to 1,10-*closo*-1,10-$C_2B_8H_{10}$, the last-but-one step being based on DSD-type rearrangement of 1,2-*closo*-1,2-$C_2B_8H_{10}$, see Holub, J.; Jelínek, T.; Janoušek, Z. *Collect. Czech. Chem. Commun.* **2002**, *67*, 949; d) Isomerization of a *nido*-$[C_2B_{10}H_{12}]^{2-}$ dianion also occurs unprecedently, via the so-called baskets and inverted *nido* molecular shapes, *closo*-type 13-vertex docosahedron being coined, see McKay, D.; Macgregor, S. A.; Welch, A. J. Isomerisation of *nido*-$[C_2B_{10}H_{12}]^{2-}$ Dianions: Unprecedented Rearrangements and New Structural Motifs in Carborane Cluster Chemistry. *Chem. Sci.* **2015**, *6*, 3117 -3128.

24. Shameena, O.; Pathak, B.; Jemmis, E. D. Theoretical Study of the Reaction of $B_{20}H_{16}$ with MeCN: *Closo/Closo* to *Closo/Nido* Conversion. *Inorg. Chem.* **2008**, *47*, 4375 - 4382.

25. McKee, M. L., In *Challenges and Advances in Computational Chemistry and Physics*, Vol. 20 (Boron The Fifth Element); Hnyk, D., McKee, M., Eds., Springer: Dordrecht, The Netherlands, 2016, pp 121-138.

26. a) For recent examples, see: Fanfrlík, J.; Přáda, A.; Padělková, Z.; Pecina, A.; Macháček, J.; Lepšík, M.; Holub, J.; Růžička, A.; Hnyk, D.; Hobza, P. The Dominant Role of Chalcogen Bonding in the Crystal Packing of 2D/3D Aromatics. *Angew. Chem. Int. Ed.* **2014**, *53*, 10139 - 10142; b) Pecina, A.; Lepšík, M.; Hnyk, D.; Hobza, P.; Fanfrlík, J. Chalcogen and Pnicogen Bonds in Complexes of Neutral Icosahedral and Biccaped Square – Antiprismatic Heteroboranes. *J. Phys. Chem. A.* **2015**, *119*, 1388 - 1395; c) Fanfrlík, J.; Holub, J.; Růžičková, Z.; Řezáč, J.; Lane, P. D.; Wann, D. A.; Hnyk, D.; Růžička, A.; Hobza, P. Competition Between Halogen, Hydrogen and

Dihydrogen Bonding in Brominated Carboranes. *Chem. Phys. Chem.*, DOI: 10.1002/cphc.201600848

For Table of Contents Only Substituted derivatives of *nido*-5,6-$C_2B_8H_{12}$ undergo extensive rearrangement on deprotonation, for which a new cage rearrangement mechanism has been proposed.